RSC Advances

PAPER

View Article Online
View Journal | View Issue

Cite this: *RSC Adv.*, 2015, **5**, 40012

Application of combined plasma-catalytic method for carbon particulate matter (PM) removal

Lu-Jie Liu, Xiang-Xiang Li, Hui Wang, Bo Xue, Xiao-Ming Zheng and Min Chen*

The carbon particulate matter (PM) generated by diesel engine emissions has attracted world-wide attention because it has a remarkable impact on air quality and the human body. Therefore, research on the removal of carbon PM has attracted increasing interest recently. Additionally, oxidative removal of carbon PM requires high temperature due to its high activation energy. In this research, a promising technology of nonthermal plasma (NTP) combined with catalytic oxidation is reported. The effective removal of carbon PM under NTP conditions by the synergy of combining plasma with MnO_x/CeO_2 catalysts at low temperatures was reported in this paper. The removal efficiency of carbon PM on MnO_x/CeO_2 catalysts (Mn loading 5.0 wt%) can be as high as 85.2% and 94.3% at 20 °C and 200 °C respectively, at the discharge power of 18.0 W and air flow rate of 30 mL min^{-1}. Moderate reaction conditions with low temperature but high removal efficiency are the advantages of the decomposition of carbon PM in a dielectric barrier discharge (DBD) reactor. It is proposed that reactive oxygen species produced under NTP conditions are responsible for carbon PM converting into CO_2. Furthermore, various parameters such as temperature, discharge power and air flow rate under NTP were investigated in the present paper, as well as the reaction process of NTP. Meanwhile, the MnO_x/CeO_2 catalysts were also characterized by XRD and TEM techniques.

Received 5th November 2014
Accepted 24th April 2015

DOI: 10.1039/c4ra13662d

www.rsc.org/advances

Introduction

Solid carbon particles such as soot, char and coke generated by gasification and combustion of coal, heavy oil, and diesel fuel, require high activation energy compared to that of a gaseous or liquid product.[1] In particular, carbon PM, emitted from diesel engine, is considered to be one of the most hazardous materials to air quality and human health.[2–4] However, removal of carbon PM is quite difficult based on current techniques, since the oxidative removal of carbon PM is usually carried out under an oxygen-rich environment in which the temperature can be reached as high as 600–700 °C due to its high activation energy. Three kinds of catalysts, the transition metal catalysts,[5–7] the spinel-type catalysts,[8–10] and the perovskite-type catalysts[11–14] have been applied in the catalytic combustion for removal of carbon PM. Among those catalysts, the perovskite-type catalysts show the best catalytic performance, but problems associated with a high temperature of 400 °C towards the formation of spinel structure have hindered its further development in removal of carbon PM.[15] Recently, solid oxides such as cerium oxide have been investigated in the catalytic oxidation at lower temperature. Some modified CeO_2 oxides catalyze oxidation of carbon PM mainly because of its function of promoting evolution of lattice oxygen.[16–19] Moreover, manganese oxides have been reported as the most efficient transition-metal oxide catalysts for catalytic disposal of pollutants and CeO_2 plays an important role as a support owing to its storage capacity of oxygen and thermal stability.[20–22] Accordingly, of these two substances, manganese oxides and cerium oxide were chosen and prepared as catalysts in this work.

Furthermore, nonthermal plasma could activate molecules including PM, hydrocarbons, and NO_x at room temperature.[23,24] Thus, extensive application of NTP has been reported in chemical synthesis,[25] removal of environmental pollutants such as volatile organic compounds (VOCs),[26,27] and fabrication of materials.[28] Consequently, moderate reacting conditions with low temperature and high removal efficiency are the advantages of decomposition of carbon PM in NTP. It is proposed that reactive oxygen species such as (O_3, active molecule of N_2 and O_2, O^+, O^-, O(1D), O(3P), and electrons)[29–32] produced under NTP conditions are responsible for carbon PM converted into CO_2. Catalytic oxidation of carbon PM with plasma assisted is the most economic approaches because of its lower temperature and excellent selectivity towards the formation of CO_2.

Therefore, a combined method of nonthermal plasma-catalytic reaction has been used in the removal of carbon PM. In this article, we present the results of catalytic oxidation carbon PM on MnO_x/CeO_2 catalysts under NTP conditions. DBD is chosen as the reactor because it can produce high concentrations of reactive oxygen species which could oxidize the carbon PM to CO_2 efficiently at lower temperature. Additionally,

Institute of Catalysis, Department of Chemistry, Zhejiang University (Xixi Campus), Hangzhou 310028, China. E-mail: chenmin@zju.edu.cn

both a combined plasma-catalytic method and reaction process of NTP were investigated.

Experimental

1. Preparation of catalyst

A series of MnO_x/CeO_2 catalysts with different manganese ratio, were prepared by impregnation method. The support of CeO_2 was dried for 2 h at 110 °C, manganese acetate solution was dropwise added. Then it was aged at ambient temperature for 12 h, followed by calcination at 500 °C for 4 h in the air atmosphere. The obtained catalysts were named as MnO_x/CeO_2.

In this paper, Printex U carbon powder was used as the substitute for carbon PM in diesel engine emissions. The carbon powder was made up of small spherical carbon particles (10–80 nm). It was subjected to chemical analyses in order to assess the solid phase emissions such as solid particulate or soot from diesel. The sample ratio of catalyst and U carbon powder was 2 : 1000 and these were prepared by mechanical grind method. All the samples were passed by the procedures of grounding fully, pressing, and sieved to 20–40 mesh size pellets.

2. Combined plasma-catalytic reactions

The experiments were carried out in a dielectric barrier discharge (DBD) reactor connected to a high-voltage power supply (Fig. 1). In the configuration of the DBD reactor, a quartz tube (i.d. 8.0 mm) was used as the reactor as well as the dielectric barrier, and also a stainless steel rod (o.d. 3.0 mm) was applied as the high-voltage electrode. At the same time, the stainless steel net wrapped on the outer surface of the quartz tube and was employed as the grounding electrode. A high-voltage power was used to control the discharge in the reactor. Discharge power was measured by the V-Q Lissajous program. The temperature of the reactor was measured by a thermocouple attached at the surface of the quartz tube reactor wall and controlled by an outer electrical heater. The sample pellets (20–40 mesh, 0.5 g) were filled in the interior of the discharge zone. Thus, a combined discharge plasma catalytic process can be carried out in this equipment. 0.5 g sample (20–40 mesh) was pretreated at 500 °C for 60 minutes in N_2 flow before experiment, and then cooled it to ambient temperature. Then a flowing mixed gas (21% O_2 and 79% N_2) was introduced into the dielectric DBD reactor in which the total flow rate was controlled at 30 mL min^{-1},and simultaneously, the stage of discharge began. This discharge process just lasted several minutes at ambient temperature.

For comparison, the catalytic mode for the removal of carbon PM was carried out under the same conditions without discharge. The products of the reaction, such as CO and CO_2, were detected on a line gas chromatography (GC-1690, keqiao, china) with a FID attachment. The PM removal on the measurements was calculated as follows:

$$\text{PM conversion } [\%] = [c(\text{CO}) + c(\text{CO}_2)]/c(\text{PM}) \times 100\% \quad (1)$$

3. Catalysts characterization

Structural characterizations of the samples were performed using X-ray diffraction (XRD). The XRD patterns were recorded on a Rigaku D/max-IIIB instrument using CuKα radiation (40 kV and 40 mA). The phase analysis was determined from XRD patterns using the MDI-JADE-5 program. Transmission electron microscopy (TEM) images were acquired with a HT-7700 electron microscope.

Results and discussion

1. Removal efficiency of carbon PM over different catalysts

Table 1 exhibits the removal efficiency of carbon PM over different catalysts such as Al_2O_3, CeO_2, MnO_x/Al_2O_3 and MnO_x/CeO_2 at the temperature range from 20 to 200 °C. Under NTP condition, as shown in Table 1, it demonstrates no carbon PM removal efficiency on those catalysts in the absence of NTP condition during this temperature range. This result shows that it is difficult to oxide carbon PM only by the catalytic combustion since oxidation of PM requires a high temperature. However, with the presence of nonthermal plasma (NTP) technologies and MnO_x/CeO_2 catalyst applied in plasma, a significant PM removal efficiency can be observed. On the MnO_x/CeO_2 (Mn loading 5.0 wt%) catalyst, the carbon PM removal efficiency reaches to 85.2% at 20 °C and 94.3% at 200 °C, respectively. This result indicates that by using NTP, the reactant molecules can be easily activated and dissociated at ambient temperature. Similarly, over other catalysts, effective carbon PM removal efficiency is obtained as well during combined plasma-catalytic process. At 200 °C, the carbon PM removal efficiency over MnO_x/Al_2O_3 catalyst is about 76.2%, and reaches 71.0% for CeO_2 and 25.5% for Al_2O_3. Among all catalysts, MnO_x/CeO_2 catalyst shows

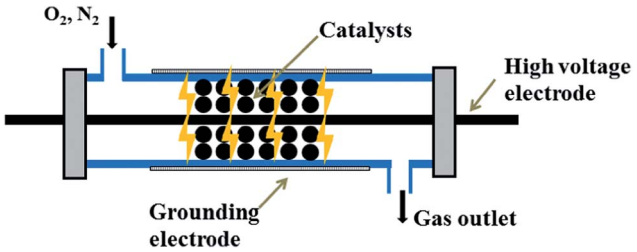

Fig. 1 The schematic diagram of the experimental setup.

Table 1 The removal efficiency of carbon PM over different catalysts at different temperature[a]

	Catalyst			
Temperature/°C	Al_2O_3	CeO_2	MnO_x/Al_2O_3	MnO_x/CeO_2
20	23.8%	23.4%	35.1%	85.2%
100	24.9%	64.1%	68.0%	87.4%
200	25.5%	71.0%	76.2%	94.3%

[a] Reaction conditions: $m_{cat.}$ = 0.50 g, total flow rate at 30 mL min^{-1}, discharge power at 18.0 W.

the highest carbon PM removal efficiency. This combined plasma-catalytic process is possible due to the fact that various oxygen atoms generated by plasma discharges play an important function in breaking C–C bonds, which results in the oxidation of graphite. These oxygen atoms are the main reactants that can react with carbon PM to convert them into CO and CO_2.[33] In the reaction process, the O_2 is converted to O^- that reacts with O_2 to generate O_3. The observed synergistic catalytic effect is owing to the fact that with manganese oxide supported on CeO_2, more oxygen can be joined in the redox cycle.[34] On the other hand, the active species generated in the discharge zone by the nonthermal plasma (NTP) are much easier for adsorption and dissociation on the surface of catalyst. As a result, radical species can reach on the surface of catalyst and participate in the reaction.

Furthermore, during the experiment, only CO_2 can be detected with no other products such as CO detected by chromatography in the effluence, indicating the main component of carbon PM is pure graphite structure.[24] It may be due to the fact that active species generated in the combined plasma-catalytic process are contributing to accelerate the reaction of carbon converted into CO and CO_2.

2. The activity of series of CeO_2-supported MnO_x catalysts

Fig. 2 demonstrates the effect of the Mn loading (2.5%, 5.0%, 7.5%) on the catalytic performance of MnO_x/CeO_2 catalysts. The removal efficiency of carbon PM increases with Mn loaded, but it reaches a highest value on 5.0% MnO_x/CeO_2 catalyst. This trend may be attributed to the formation of bulk manganese particles which will decrease catalytic activity when the MnO_x content is over 7.5%.[34]

3. The morphology of the 5% MnO_x/CeO_2 catalyst

XRD was used for direct observations of the catalyst. Three patterns, representing of CeO_2, 5% MnO_x/CeO_2 catalyst before and after combined plasma-catalytic reaction are presented in Fig. 3. On the CeO_2 sample (A), the diffraction peaks due to cubic CeO_2 phase are detected. On the 5% MnO_x/CeO_2 catalysts before and after reaction (B and C), no diffraction peak, characteristic of the manganese oxide could be observed except the CeO_2 phase, indicating the MnO_x was in high dispersion on the CeO_2 surface. This could be explained by the fact that the XRD technique could not detect very small crystallites (usually <3 nm).[35] Meanwhile, XRD patterns of MnO_x/CeO_2 before and after reaction showed that the catalyst still kept its crystalline structure after the plasma reaction.

Moreover, TEM was used for direct observations of the 5% MnO_x/CeO_2 catalysts. The surface morphology of the 5% MnO_x/CeO_2 catalysts before and after NTP reaction is clearly shown in Fig. 4. It can be seen that the catalyst shows no evident changes after nonthermal plasma reaction, indicating the 5% MnO_x/CeO_2 catalyst has high stability and can be recycled. Both results (XRD and TEM) suggest that the performance of 5% MnO_x/CeO_2 catalyst is stable under the plasma discharge conditions.

4. Effect of discharge power and flow velocity in plasma-catalytic process

Since the parameter affects the reaction greatly, the characteristic information such as flow rate and discharge power was investigated. Fig. 5(a) shows the conversion of carbon PM in O_2 plasma on 5% MnO_x/CeO_2 as a function of flow rate at the range from 30 to 90 mL min^{-1}. It is clear that the conversion of carbon PM to CO_2 shows a declining trend with the increasing of flow rate. It reaches the maximum at the lower flow rate of 30 mL min^{-1}, and then drops dramatically at 90 mL min^{-1}, indicating the condition of 30 mL min^{-1} in flow rate is proved to be the suitable condition for the removal of carbon PM in NTP-catalytic reaction, which can be interpreted that more and more active particles are generated in the discharge zone of plasma under appropriate flow rate conditions. Moreover, with the increase of flow rate, the effective collisions between active particles and reactant molecules are inevitably reduced as the flow rate of

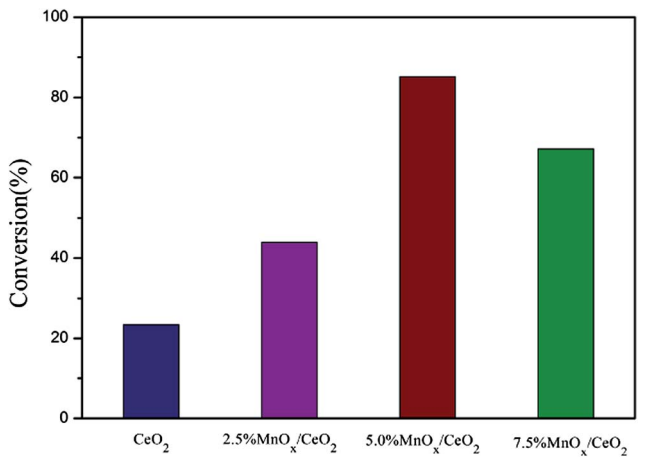

Fig. 2 Removal properties of carbon PM as a function of different Mn loadings on MnO_x/CeO_2 catalysts (reaction conditions: room temperature, 30 mL min^{-1} flow rate of the air, discharge power at 18.0 W).

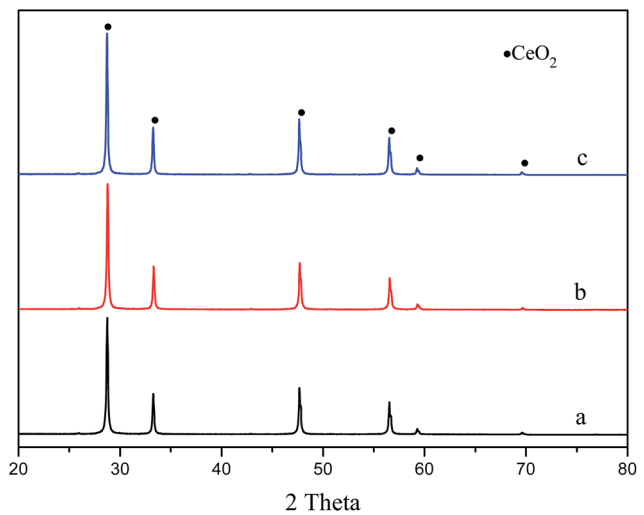

Fig. 3 XRD patterns of (a) CeO_2, 5% MnO_x/CeO_2 catalyst (b) before and (c) after reaction.

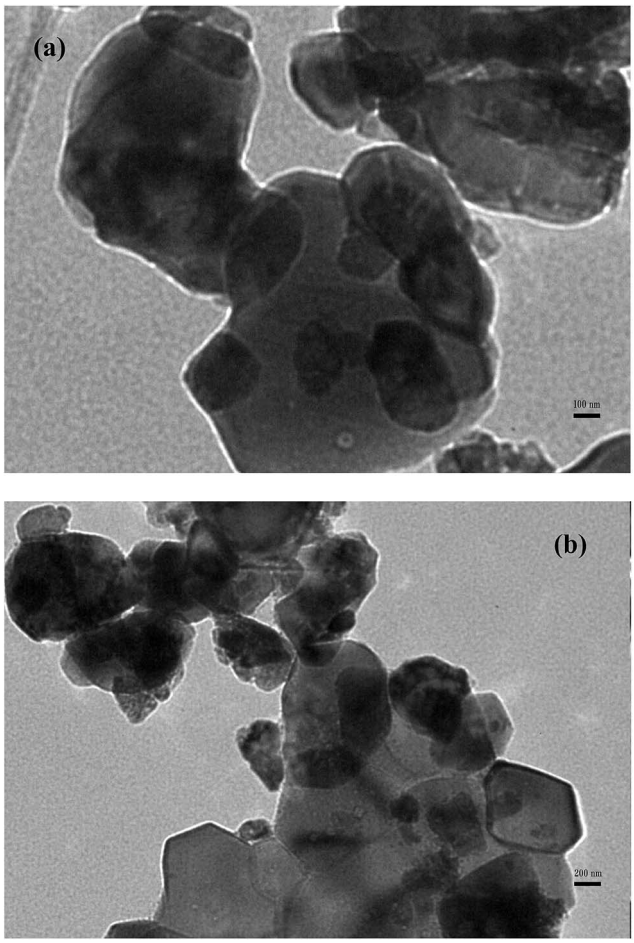

Fig. 4 TEM photograph of 5% MnO_x/CeO_2 catalyst (a) before and (b) after reaction; (reaction condition: total flow rate at 30 mL min^{-1}, discharge power at 18.0 W and temperature at 200 °C).

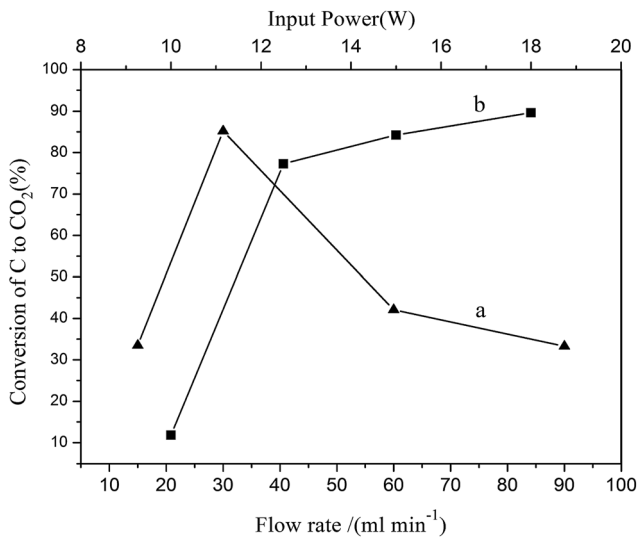

Fig. 5 Removal efficiency of carbon PM as a function of (a) flow rate and (b) discharge power over MnO_x/CeO_2 catalyst (reaction condition (a): ambient temperature, discharge power at 18.0 W; (b): ambient temperature, 30 mL min^{-1} flow rate of the air).

reactant gas increased. Thus, the following experiments were carried out at the condition of flow rate of 30 mL min^{-1}.

Additionally, the discharge power is an important parameter for plasma chemistry. The influence of the discharge power on carbon PM oxidation in NTP is also shown in Fig. 4(b). It shows an opposite trend in that of flow rate. Obviously, at the range of discharge power from 10.0 to 18.0 W, the conversion of carbon PM to CO_2 greatly improves with the increasing of discharge power. This is due to the fact that higher discharge power is able to supply more electrons with sufficient energy to activate the carbon PM particle. As a result, the active particle density can be improved and then the oxidation of carbon PM will be sped up.

5. Effect of reaction temperature and time in plasma-catalytic process

The effect of reaction temperature and time on plasma removal of PM over CeO_2 and 5% MnO_x/CeO_2 catalyst are illustrated in Fig. 6. As can be seen from Fig. 6, carbon PM removal efficiency is clearly influenced by both temperature and time. The carbon PM removal efficiency over CeO_2 at ambient temperature are quite low and with the time increasing to 25 minutes, the PM removal efficiency is still lower to 20%. However, for 5% MnO_x/CeO_2 catalyst, at the same reaction time, the PM removal rate reaches 80%, indicating the carbon PM removal is improved significantly. This result suggests that by supported manganese oxide on CeO_2, it may be enter into ceria lattice and improves the oxygen storage capacity of ceria as well as the oxygen mobility on the surface of the mixed oxides.[21] It is obviously on 5% MnO_x/CeO_2 catalyst, when temperature is higher to 200 °C, the reaction happens more rapidly. The removal of carbon PM is higher than 90% in 10 minutes.

6. Reaction process for carbon PM removal under plasma discharge conditions

The mechanism of carbon PM removed under plasma discharge conditions is not clear. From the fact that oxidation products is carbon dioxide, the nonthermal plasma reaction processing for

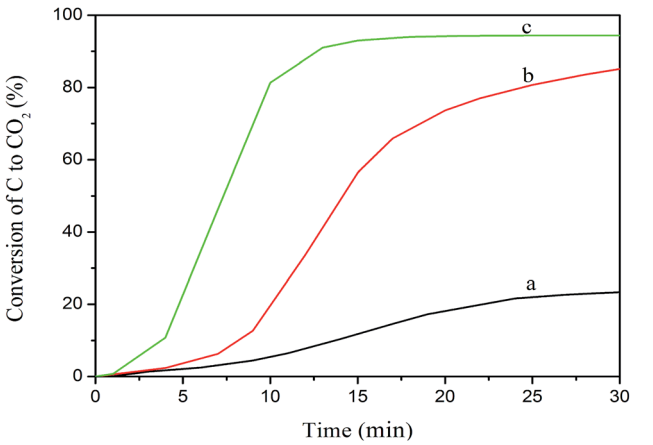

Fig. 6 PM removal as a function of reaction time on catalysts: (a) CeO_2 at ambient temperature, (b) 5% MnO_x/CeO_2 at ambient temperature, (c) 5% MnO_x/CeO_2 at 200 °C.

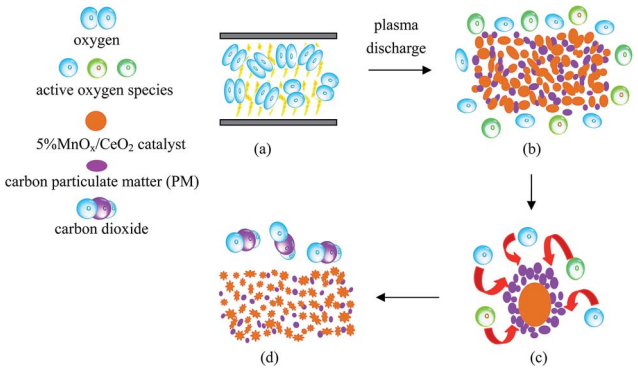

Fig. 7 Nonthermal plasma (NTP) reaction process for oxidation of carbon PM to CO_2.

oxidation of carbon PM to CO_2 may be presumably in Fig. 7. Firstly, activated radical oxygen species induced by NTP, such as O_3, O^-, O(1D), O(3P), are generated. With the synergistic effect of MnO_x/CeO_2 catalyst, some of them are adsorbed on the surface of the MnO_x/CeO_2 catalyst by diffusion and more effective collisions happen between active particle of catalyst and carbon PM particle. These active oxygen species contact with carbon PM and react, then forming large amounts CO radicals efficiently. Finally, the target product CO_2 is produced, with the carbon PM incinerated, after CO radicals combine with the former active oxygen species.

Conclusions

The combined plasma-catalytic process may be an efficient way for the removal of carbon PM. 5% MnO_x/CeO_2 has been demonstrated to be an efficient catalyst in the plasma-catalytic reaction for carbon PM converted into CO_2. The synergistic effect between the plasma and the catalyst is mainly due to the active oxygen species yielded by NTP. These active species on the catalyst also play a role in the reaction of carbon PM removal. As a result, in this process, carbon PM removal could achieve 85.2% at ambient temperature. Due to the presence of nonthermal plasma (NTP), the temperature of the reaction is lower than that in traditional catalytic combustion mode.

Acknowledgements

The support of 973 Program (2013CB228104) of China is greatly appreciated.

References

1 Y. Sekine, H. Koyama, M. Matsukata and E. Kikuchi, Plasma-assisted oxidation of carbon particle by lattice oxygen on/in oxide catalyst, *Fuel*, 2013, **103**, 2–6.
2 D. W. Dockery and P. H. Stone, Cardiovascular risks from fine particulate air pollution, *N. Engl. J. Med.*, 2007, **356**(5), 511–513.
3 B. Giechaskiel, B. Alföldy and Y. Drossinos, A metric for health effects studies of diesel exhaust particles, *J. Aerosol Sci.*, 2009, **40**(8), 639–651.
4 Y. Q. Sheng, Y. Zhou, H. F. Lu, Z. K. Zhang and Y. F. Chen, Soot combustion performance and H_2-TPR study on ceria-based mixed oxides, *Chin. J. Catal.*, 2013, **34**(3), 567–577.
5 K. Hinot, H. Burtscher, A. P. Weber and G. Kasper, The effect of the contact between platinum and soot particles on the catalytic oxidation of soot deposits on a diesel particle filter, *Appl. Catal., B*, 2007, **71**(3–4), 271–278.
6 Z. P. Wang, Z. Jiang and W. F. Shangguan, Simultaneous catalytic removal of NO_x and soot particulate over Co–Al mixed oxide catalysts derived from hydrotalcites, *Catal. Commun.*, 2007, **8**(11), 1659–1664.
7 X. D. Wu, Q. Liang, D. Weng and Z. X. Lu, The catalytic activity of CuO–CeO_2 mixed oxides for diesel soot oxidation with a NO/O_2 mixture, *Catal. Commun.*, 2007, **8**(12), 2110–2114.
8 Q. Li, M. Meng, N. Tsubaki, X. G. Li, Z. Q. Li, Y. N. Xie, T. D. Hu and J. Zhang, Performance of K-promoted hydrotalcite-derived CoMgAlO catalysts used for soot combustion, NO_x storage and simultaneous soot-NO_x removal, *Appl. Catal., B*, 2009, **91**(1–2), 406–415.
9 W. F. Shangguan, Y. Teraoka and S. Kagawa, Simultaneous catalytic removal of NO_x and diesel soot particulates over ternary AB(2)O(4) spinel-type oxides, *Appl. Catal., B*, 1996, **8**(2), 217–227.
10 M. Zawadzki, W. Walerczyk, F. E. López-Suárez, M. J. Illan-Gomez and A. Bueno-Lopez, $CoAl_2O_4$ spinel catalyst for soot combustion with NO_x/O_2, *Catal. Commun.*, 2011, **12**(13), 1238–1241.
11 J. F. Xu, J. Liu, Z. Zhao, C. M. Xu, J. X. Zheng, A. J. Duan and G. Y. Jiang, Easy synthesis of three-dimensionally ordered macroporous $La_{1-x}K_xCoO_3$ catalysts and their high activities for the catalytic combustion of soot, *J. Catal.*, 2011, **282**(1), 1–12.
12 Y. Teraoka, K. Nakano, W. Shangguan and S. Kagawa, Simultaneous catalytic removal of nitrogen oxides and diesel soot particulate over perovskite-related oxides, *Catal. Today*, 1996, **27**(1–2), 107–113.
13 S. S. Hong and G. D. Lee, Simultaneous removal of NO and carbon particulates over lanthanoid perovskite-type catalysts, *Catal. Today*, 2000, **63**(2–4), 397–404.
14 Y. Teraoka, K. Kanada and S. Kagawa, Synthesis of La–K–Mn–O perovskite-type oxides and their catalytic property for simultaneous removal of NO_x and diesel soot particulates, *Appl. Catal., B*, 2001, **34**(1), 73–78.
15 Z. Q. Li, M. Meng, Q. A. Li, Y. N. Xie, T. D. Hu and J. Zhang, Fe-substituted nanometric $La_{0.9}K_{0.1}Co_{1-x}Fe_xO_3$-delta perovskite catalysts used for soot combustion, NO_x storage and simultaneous catalytic removal of soot and NO_x, *Chem. Eng. J.*, 2010, **164**(1), 98–105.
16 A. Bueno-Lopéz, K. Krishna, M. Makkee and J. A. Moulijn, Enhanced soot oxidation by lattice oxygen via La^{3+}-doped CeO_2, *J. Catal.*, 2005, **230**(1), 237–248.
17 K. Krishna, S. Liu, A. Bueno-Lopéz, M. Makkee and J. A. Moulijn, Potential rare earth modified CeO_2 catalysts

for soot oxidation I. Characterisation and catalytic activity with O_2, *Appl. Catal., B*, 2007, **75**(3–4), 189–200.

18 K. Harada, Y. Tsushio and A. Takami, Lowering combustion temperature of carbon particles on Pt-supported ceria series oxides, *J. Jpn. Pet. Inst.*, 2005, **48**(4), 216–222.

19 A. Takami, K. Harada and Y. Tsushio, Behavior of oxygen of cerium composite oxides on catalytic combustion of carbon particulate, *J. Jpn. Pet. Inst.*, 2007, **50**(2), 102–107.

20 E. Saab, S. Aouad, E. Abi-Aad, E. Zhilinskaya and A. Aboukais, Carbon black oxidation in the presence of Al_2O_3, CeO_2, and Mn oxide catalysts: an EPR study, *Catal. Today*, 2007, **119**(1–4), 286–290.

21 X. D. Wu, S. Liu, D. Weng, F. Lin and R. Ran, MnO_x–CeO_2–Al_2O_3 mixed oxides for soot oxidation: activity and thermal stability, *J. Hazard. Mater.*, 2011, **187**(1–3), 283–290.

22 H. Muroyama, S. Hano, T. Matsui and K. Eguchi, Catalytic soot combustion over CeO_2-based oxides, *Catal. Today*, 2010, **153**(3–4), 133–135.

23 H. Wang, Q. Q. Yu, T. Liu, L. P. Xiao and X. M. Zheng, NO_x storage and reduction with methane by plasma at ambient temperature, *RSC. Adv.*, 2012, **2**(12), 5094–5097.

24 C. Fushimi, K. Madokoro, S. Yao, Y. Fujioka and K. Yamada, Influence of polarity and rise time of pulse voltage waveforms on diesel particulate matter removal using an uneven dielectric barrier discharge reactor, *Plasma Chem. Plasma Process.*, 2008, **28**(4), 511–522.

25 X. S. Li, C. Shi, Y. Xu, K. J. Wang and A. M. Zhu, A process for a high yield of aromatics from the oxygen-free conversion of methane: combining plasma with Ni/HZSM-5 catalysts, *Green Chem.*, 2007, **9**(6), 647–653.

26 J. H. Niu, X. F. Yang, A. M. Zhu, L. L. Shi, Q. Sun, Y. Xu and C. Shi, Plasma-assisted selective catalytic reduction of NO_x by C_2H_2 over Co-HZSM-5 catalyst, *Catal. Commun.*, 2006, **7**(5), 297–301.

27 Q. Q. Yu, H. Wang, T. Liu, L. P. Xiao, X. Y. Jiang and X. M. Zheng, High-Efficiency Removal of NO_x Using a Combined Adsorption-Discharge Plasma Catalytic Process, *Environ. Sci. Technol.*, 2012, **46**(4), 2337–2344.

28 C. Bower, O. Zhou, W. Zhu, D. J. Werder and S. H. Jin, Nucleation and growth of carbon nanotubes by microwave plasma chemical vapor deposition, *Appl. Phys. Lett.*, 2000, **77**(17), 2767–2769.

29 J. V. Durme, J. Dewulf, C. Leys and H. V. Langenhove, Combining non-thermal plasma with heterogeneous catalysis in waste gas treatment: a review, *Appl. Catal., B*, 2008, **78**(3–4), 324–333.

30 J. Karuppiah, L. Sivachrandiran, R. Karvembu and C. Subrahmanyam, Catalytic Plasma Reactor for Abatement of Dilute Nitrobenzene, *Chin. J. Catal.*, 2011, **32**(5), 795–799.

31 F. Holzer, U. Roland and F. D. Kopinke, Combination of non-thermal plasma and heterogeneous catalysis for oxidation of volatile organic compounds Part 1. Accessibility of the intra-particle volume, *Appl. Catal., B*, 2002, **38**(3), 163–181.

32 C. Y. Chen, T. Liu, H. Wang, Q. Q. Yu, J. Fan, L. P. Xiao and X. M. Zhen, Removal of Hexanal by Non-thermal Plasma and MnO_x/gamma-Al_2O_3 Combination, *Chin. J. Catal.*, 2012, **33**(6), 941–951.

33 B. Lu, M. M. Ji, M. Wang and J. B. Lu, Plasma oxidation of benzene using DBD corona discharges, *J. Mater. Eng. Perform.*, 2008, **17**(3), 428–431.

34 Y. Liu, M. F. Luo, Z. B. Wei, Q. Xin, P. L. Ying and C. Li, Catalytic oxidation of chlorobenzene on supported manganese oxide catalysts, *Appl. Catal., B*, 2001, **29**(1), 61–67.

35 A. P. Jia, S. Y. Jiang, J. Q. Lu and M. F. Luo, Study of catalytic activity at the CuO–CeO_2 interface for CO oxidation, *J. Phys. Chem. C*, 2010, **114**(49), 21605–21610.